PLASTIC DEFORMATION IN STEEL FRAMES WITH COLUMN BASES HAVING RELATIVELY WEAK STRENGTH

M. Yokoo[1], H. Nakahara[2], M. Yamanari[3] and K. Ogawa[4]

[1] *Graduate Student, Graduate School of Science and Technology, Kumamoto University, Kumamoto, Japan*
[2] *Research Fellow, Graduate School of Science and Technology, Kumamoto University, Kumamoto, Japan*
[3] *Associate Professor, Graduate School of Science and Technology, Kumamoto University, Kumamoto, Japan*
[4] *Professor, Graduate School of Science and Technology, Kumamoto University, Kumamoto, Japan*
Email: ogawa@kumamoto-u.ac.jp, yamanari@kumamoto-u.ac.jp

ABSTRACT:

In this study, we investigate the plastic deformation in steel moment frames with column bases having a relatively weak strength. The strength of the column bases was changed at 15 steel frames that are fabricated according to the Japanese seismic design code. Numerical analyses regarding the seismic response of these frames were carried out, applying a variety of ground motions. The maximum plastic rotation, maximum increment of plastic rotation during half the vibration cycle, and cumulative plastic rotation are considered to be the parameters that represent the magnitude of plastic deformation. As a result, the cumulative plastic rotation divided by the maximum increment of the plastic rotation during half the vibration cycle of the column base increases rapidly as the strength of the column base decreases. However, for the second-floor beam ends, these values are almost constant even if the strength of the column base decreases.

KEYWORDS: Column Base, Beam, Earthquake Response, Maximum Story Drift Angle, Maximum Plastic Rotation, Performance-Based Design

1. INTRODUCTION

Hyogoken-Nanbu (Kobe) earthquake (1995) caused serious damage to modern steel building structures. Therefore, it has become imperative to perform the evaluation and improvement in the deformation capacity of beam-to-column joints and column bases. However, the number of studies focused on the ductility demand of beam ends and column bases is small at this moment.

The authors investigated the ductility demand of the beam end. In the past, it has been reported that the change in the restoring force characteristics of the column bases does not influence the maximum story drift angle when the maximum loading capacity and elastic stiffness of the first story are kept constant. Hence, the first-story drift angle is not larger than the others, regardless of the strength of the column bases if the strength and elastic stiffness of the first story are sufficient. In addition, this value can be predicted similar to in the case of the others. There is a possibility that the plastic deformation of the second-floor beam ends increases with the deformation of the frames on the first story with column bases having a relatively weak strength. The maximum story drift angle of the first story changes with not only the structural characteristics, such as the elastic stiffness, ultimate strength, and column-to-beam strength ratio, but also the input ground motions. However, from the viewpoint of performance-based design, the determination of this value at the preliminary structural design seems to be a popular choice. Hence, if the relationships between the story drift angle and plastic deformation of the column base is obvious, the ductility demand of the column base is obtained when the maximum story drift angle is given.

In this study, the relationship between the story drift angle and plastic deformation is defined according to a seismic response analysis with the strain-hardening general yield hinge method for the 15 steel frames.

2. OUTLINE OF ANALYSIS

The characteristics of the analyzed frames are listed in Table 1. All of the frames are steel moment frames consisting of rectangular hollow-section steel columns and wide-flange steel beams. The shapes of the frames are shown in Figure 2.1 (a). These are 2-, 8-, and 12-story frames in AR and BR in addition to the 4-story frame shown in Figure 2.1 (a). There are 2-, and 8-story frames in CR in addition to the 4-story frame shown in Figure 2.1 (a). These frames have the same span and span length. There are two kinds of frames, namely, Frame A and Frame B, in BRI3 and BRI9, respectively. These frames have the same number of stories, story height, span, and span length, but they are designed by different people.

Table 1. Analyzed Frames

Name	Number of stories	First natural period (s.)	Ultimate base shear coefficient
AR02	2	0.606	0.572
AR04	4	0.820	0.425
AR08	8	1.173	0.405
AR12	12	1.625	0.284
BR02	2	0.541	0.813
BR04	4	0.800	0.526
BR08	8	1.148	0.492
BR12	12	1.576	0.345
CR02	2	0.629	0.501
CR04	4	0.841	0.404
CR08	8	1.159	0.365
BRI3A	3	0.638	0.557
BRI3B	3	0.688	0.506
BRI9A	9	1.882	0.209
BRI9B	9	1.834	0.227

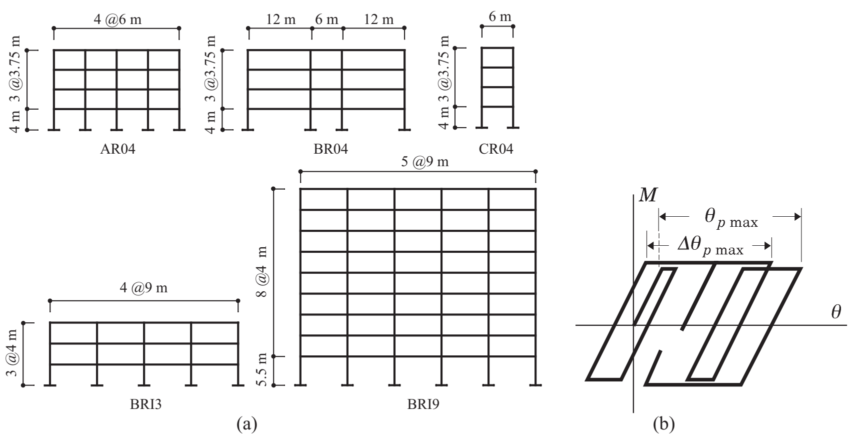

Figure 2.1: Outline of Analysis: (a) Shapes of the Frames and (b) Parameters

Suites of ground motions used in the FEMA/SAC project were used for the dynamic response analysis of the frames. They were 2 sets of 20 records that represent the probabilities 10% and 2% in 50 years in the Los Angeles area of the United States, denoted as the 10/50 and 2/50 record sets, respectively.

These frames were analyzed using the strain-hardening general yield hinge method, considering the shearing deformation of the joint panels. The strain-hardening coefficient of the members and joint panels is 0.02. The step time of the numerical integration of the seismic response analysis is 0.0002 s. Rigid–plastic rotational springs were inserted into the column bases to change the strength of the column bases without modifying their cross sections. The plastic deformation of the spring represented the deformations of the column bases. The springs have a kinematics-hardening-type restoring force characteristic rather than a slipping-type characteristic.

Although the relationship between the load and deformation is bilinear having an elastic region, the characteristic is similar to that of a rigid plastic owing to the bending stiffness of the springs, which is 1000 times larger than the value of column base. The strain-hardening coefficient of the springs is 0.00002 and it seems to be 0.02 from the viewpoint of the relationship between the column base and springs. The bending strength of the springs is based on the strength when one of the second-floor beam ends and the springs of the frames with static addition of the seismic load of the Japanese design code yield at the same time. The strength is expressed as r_B times the original value. There are six r_B values, namely, 0.2, 0.4, 0.6, 0.8, 1.0, and 1.2. In this study, the strength of the members, except for the springs, does not change if the value of r_B decreases.

The maximum of the absolute value of the plastic rotation is defined to be the maximum plastic rotation ($\theta_{p\,\max}$). Further, the maximum increment of the plastic rotation during half the cycle of vibration ($\Delta\theta_{p\,\max}$) and cumulative plastic rotation ($\Sigma\Delta\theta_p$) are used. However, in this study, the maximum plastic rotation is considered to be the most important parameter, and the responses are arranged around the part having the largest maximum plastic rotation.

3. RESULTS

3.1 Maximum Plastic Rotation of the Column Base $\theta_{p\,\max}$

Each relationship between the maximum plastic rotation ($\theta_{p\,\max}$) of the column base and maximum drift angles ($R_{\max}$) is shown in Figure 3.1 when r_B is changed to 0.2, 0.6, and 1.0.

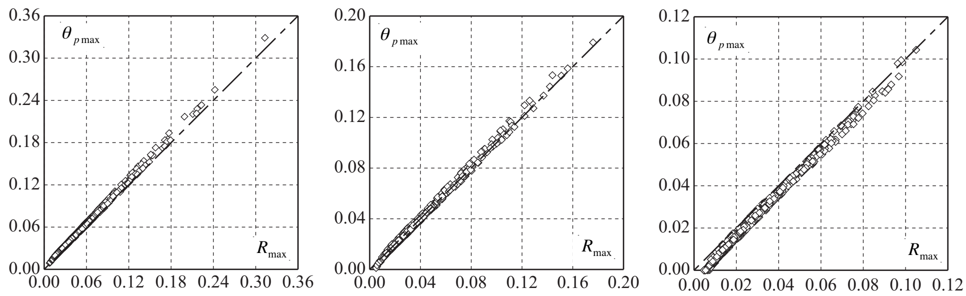

(a) $r_B = 0.2$ (b) $r_B = 0.6$ (c) $r_B = 1.0$

Figure 3.1: Relationship between $\theta_{p\max}$ and $R_{\max}$ of the Column Bases

According to Figure 3.1, $\theta_{p\,\max}$ can be approximated to $R_{\max}$. However, $\theta_{p\,\max}$ tends to be more than $R_{\max}$ when $r_B = 0.2$, while $\theta_{p\,\max}$ tends to less than $R_{\max}$ when $r_B = 1.0$. According to Figure 3.1 (a) and (b), there are many extreme drift angles that exceed 0.1 radians. The reason is that the strength of all the members in the analyzed frames, except for the spring, does not change even if r_B is changed in the analyzed frames of this

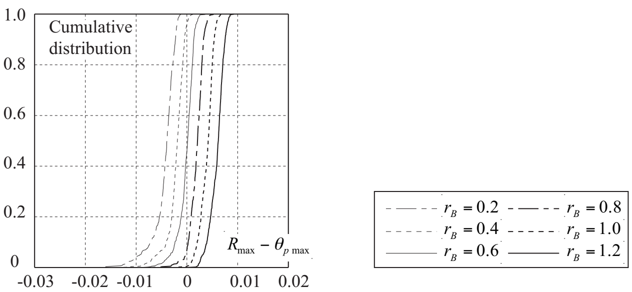

Figure 3.2: Cumulative Distribution: $R_{\max} - \theta_{\max}$ of the Column Bases

study. Therefore, if the strength of the rotational springs decreases with a decrease in r_B, the plastic deformation increases as the strength of the first story decreases. However, for actual frames, the strength of the first story is sufficient such that the stress on all parts of the frames is less than the allowable stress and there is sufficient shearing strength. Therefore, an increment in the first-story drift angle and plastic deformation of the column base does not occur. The cumulative distribution of the difference in $R_{\max}$ and $\theta_{p\max}$ is shown in Figure 3.2. It decreases by 0.002 for every decrease of 0.2 in r_B. When the column base yields earlier than the other members when r_B is less than 1.0, the column of the first story is deformed without the consideration of the deformation of the beams and joint panels, as shown in Figure 3.3 (a).

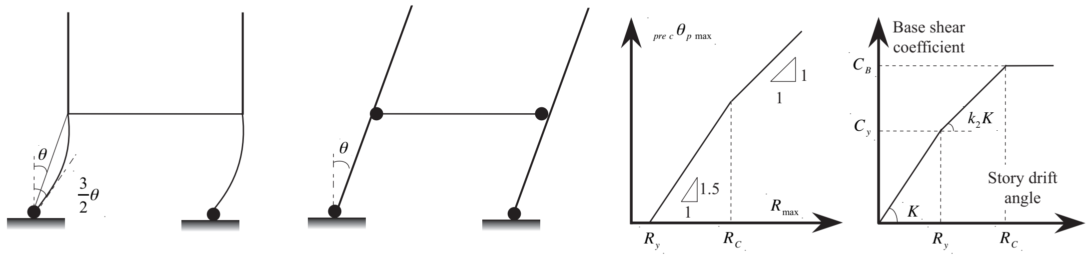

(a) (b) (c) (d)

Figure 3.3: Plastic Deformation of Column Base: (a) Behavior of the Second Branching and (b) Behavior of the Third Branching
Prediction of the Plastic Deformation of the Column Base: (c) Relationship between $R_{\max}$ and ${}_{pre\,c}\theta_{p\max}$ and (d) Relationship between the Story drift Angle and Shear Coefficient

The increment of the plastic rotation of the column base is larger than the increment of the story drift angle. Then, the increment of the plastic rotation is 1.5 times larger than that of the story drift angle. This is the reason why $\theta_{p\max}$ is larger than $R_{\max}$ at the frames when r_B is less than 1.0. Moreover, the deformation advances and the top of the column of the first story (e.g., beam and joint panels), such as that shown in Figure 3.3 (b), after this increment of the plastic rotation is equal to that of the story drift angle. Further, the relationship between the prediction of the maximum plastic rotation (${}_{pre\,c}\theta_{p\max}$) and $R_{\max}$ is shown in Figure 3.3 (c) with the story drift angle when the collapse mechanism is formed and the base shear coefficient reaches its ultimate value (R_C). Therefore,

$${}_{pre\,c}\theta_{p\max} = \min\left\{1.5\left(R_{\max} - R_y\right), 1.5\left(R_C - R_y\right) + R_{\max} - R_C\right\} \tag{3.1}$$

The relationship between the first-story drift angle and the base shear coefficient is trilinear, such as that shown in Figure 3.3 (d). Then R_C is,

$$R_C = \left(\frac{C_B - C_y}{k_2\, C_y} + 1\right) R_y \tag{3.2}$$

The ultimate base shear coefficient (C_B) is the maximum when the horizontal displacement of the frames with the designed seismic load of Japanese design code is equal to 1/50 of the height of the frames. Here, R_y is the first-story drift angle and C_y is the base shear coefficient when the plastic hinges are first formed under an earthquake. These values for the frames with rotational springs are multiplied by r_B when r_B is less than 1.0. For a value of 1.2, these values are the same in the case of r_B = 1.0. k_2 is the stiffness ratio of the second branch shown in Figure 3.3 (d). Only the column bases yield (Figure 3.3(a)) at the second branch. Then, the stiffness of relationship between story drift and shearing force with the deformation of the column base is one-fourth larger than one in the elastic range. Hence, the ratio of the deformation of the column in the elastic deformation is γ_C. Then k_2 is,

$$k_2 = \frac{1}{4\gamma_C + (1-\gamma_C)} \tag{3.3}$$

When γ_C is 0.5, k_2 is 0.4.

$$k_2 = 0.4 \tag{3.4}$$

With Eqn. (3.2) and Eqn. (3.4), ${}_{pre\,c}\theta_{p\max}$ when r_B is changed from 0.2 and 1.2 were calculated using Eqn. (3.1). Further, the cumulative distribution of the difference in ${}_{pre\,c}\theta_{p\max}$ and $\theta_{p\max}$ is shown in Figure 3.4.

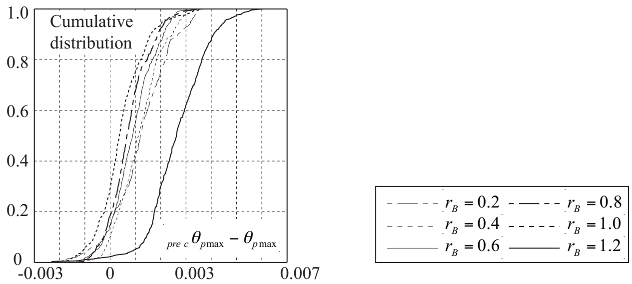

Figure 3.4: Cumulative Distribution: ${}_{pre\,c}\theta_{p\max} - \theta_{p\max}$ of the Column Base

3.2 Maximum Plastic Rotation of the Second-Floor Beam End $\theta_{p\max}$

Each relationship between maximum plastic rotation of the second floor beam end ($\theta_{p\max}$) and the maximum drift angle ($R_{\max}$) is shown in Figure 3.5, when r_B is changed to 0.2, 0.6, and 1.0.

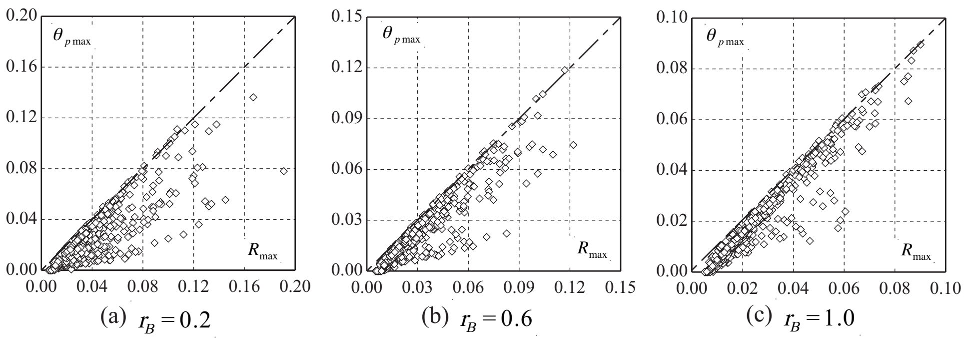

Figure 3.5: Relationship between $\theta_{p\max}$ and $R_{\max}$ of the Second-Floor Beam End.

In this case, $R_{\max}$ denotes the average of the first- and second-story drift angles. According to Figure 3.5, $\theta_{p\max}$ are uneven $R_{\max}$ compared with in the case of the column base. The cumulative distribution of the difference in $R_{\max}$ and $\theta_{p\max}$ is shown in Figure 3.6 (a). It increases as r_B decreases. This increase is approximately from 0 to 0.05. Although this difference is larger than the one for the column base, $R_{\max}$ can be approximated to the upper limit of $\theta_{p\max}$. The relationship between $\theta_{p\max}$ and the prediction of the maximum plastic rotation of the second-floor beam end (${}_{pre\,b}\theta_{p\max}$) was considered similar to the case of the column base. However, the story drift angle when the plastic hinges were formed at both the ends is the necessary when Eqn. (3.1) is employed. According to Figure 3.5, $\theta_{p\max}$ can be approximated to $R_{\max}$ in the range where $R_{\max}$ is large.

$${}_{pre\,b}\theta_{p\max} = R_{\max} \tag{3.5}$$

This equation implies that the story drift angle when the plastic hinges were formed at both the ends is three times R_y; thereafter, the increment in the plastic hinges is equal to the increment in the story drift angle. That is,

$$ {}_{pre\,b}\theta_{p\max} = \min\left\{1.5\left(R_{\max} - R_y\right), R_{\max}\right\} \tag{3.6} $$

The cumulative distribution of the differences in ${}_{pre\,b}\theta_{p\max}$ and $\theta_{p\max}$ is shown in Figure 3.6 (b). This difference increases as r_B decreases.

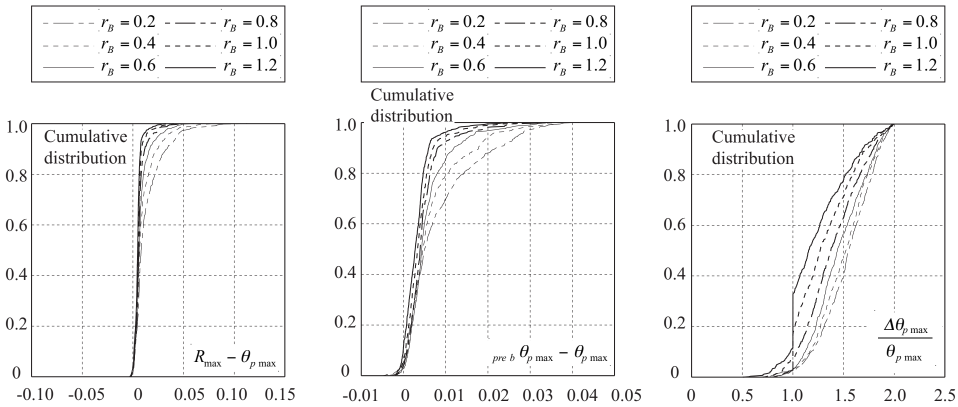

(a) (b) (c)

Figure 3.6: Cumulative Distribution for (a) $R_{\max} - \theta_{p\max}$ of the Second-Floor Beam end, (b) ${}_{pre\,b}\theta_{p\max} - \theta_{p\max}$ of the Second-Floor Beam End, and (c) $\Delta\theta_{p\max} / \theta_{p\max}$ of the Column Base

3.3 Maximum Increment of Plastic Rotation of the Column Base $\Delta\theta_{p\max}$

The cumulative distribution of the values in which the maximum increment of the plastic rotation ($\Delta\theta_{p\max}$) of the column base divided by the maximum plastic rotation ($\theta_{p\max}$) of the column base, as shown in Figure 3.6 (c). These values are between 1.0 and 2.0. $\Delta\theta_{p\max} / \theta_{p\max}$ increases as r_B decreases.

3.4 Maximum Increment of Plastic Rotation of the Second-Floor Beams End $\Delta\theta_{p\max}$

The cumulative distribution of the values in which the maximum increment of plastic rotation ($\Delta\theta_{p\max}$) of the second-floor beam end divided by the maximum plastic rotation ($\theta_{p\max}$) of the second-floor beam ends is shown in Figure 3.7. The values are between 1.0 and 1.5. $\Delta\theta_{p\max} / \theta_{p\max}$ increases as r_B decreases.

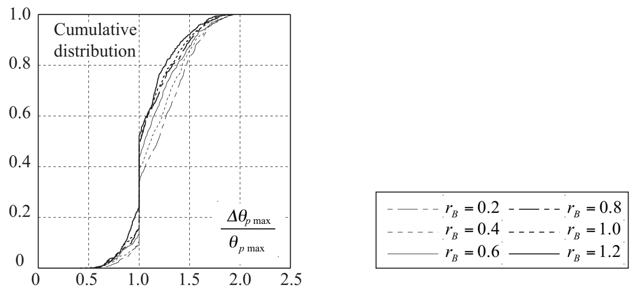

Figure 3.7: Cumulative Distribution $\Delta\theta_{p\max} / \theta_{p\max}$ of the Second-Floor Beam End

3.5 Cumulative Plastic Rotation of the Column Base $\Sigma\Delta\theta_p$

Each relationship between the cumulative plastic rotation ($\Sigma\Delta\theta_p$) of the column base and the maximum increment of the plastic rotation ($\Delta\theta_{p\max}$) of the column base is shown in Figure 3.8, when r_B is changed to 0.2, 0.6, and 1.0. The cumulative distribution of these values in which $\Sigma\Delta\theta_p$ of the column base divided by $\Delta\theta_{p\max}$ of the column base is shown in Figure 3.9. $\Sigma\Delta\theta_p / \Delta\theta_{p\max}$ increases rapidly as r_B decreases. Therefore, the upper limit cannot be predicted as long as the strength of the column base was given.

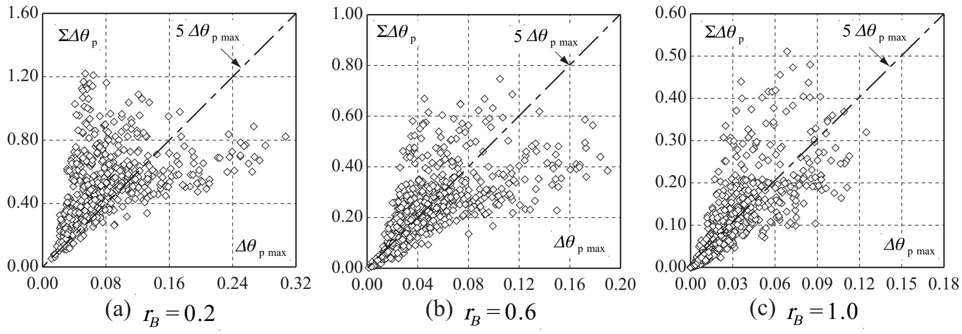

Figure 3.8: Relationship between $\Sigma\Delta\theta_p$ and $\Delta\theta_{p\,\max}$ of the Column Base

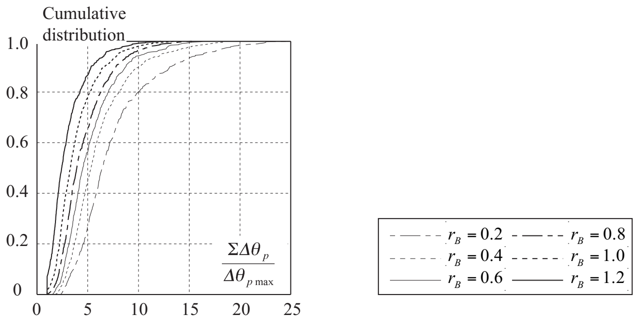

Figure 3.9: Cumulative Distribution $\Sigma\Delta\theta_p / \Delta\theta_{p\,\max}$ of the Column Base

3.6 Cumulative Plastic Rotation of the Second-Floor Beam End $\Sigma\Delta\theta_p$

Each relationship between the cumulative plastic rotation ($\Sigma\Delta\theta_p$) of the second-floor beam end and the maximum increment of the plastic rotation ($\Delta\theta_{p\,\max}$) of the second-floor beam end is shown in Figure 3.10, when r_B is changed to 0.2, 0.6, and 1.0. The cumulative distribution of the values in which $\Sigma\Delta\theta_p$ of the second-floor beam end divided by $\Delta\theta_{p\,\max}$ of the second-floor beam end is shown in Figure 3.11. These values are between 1.0 and 10 for all of the values of r_B. In addition, approximately 80% of these values are less than 5.0. Therefore, their upper limits can be approximated to 5.0. Further, $\Sigma\Delta\theta_p / \Delta\theta_{p\,\max}$ is constant even if r_B decreases.

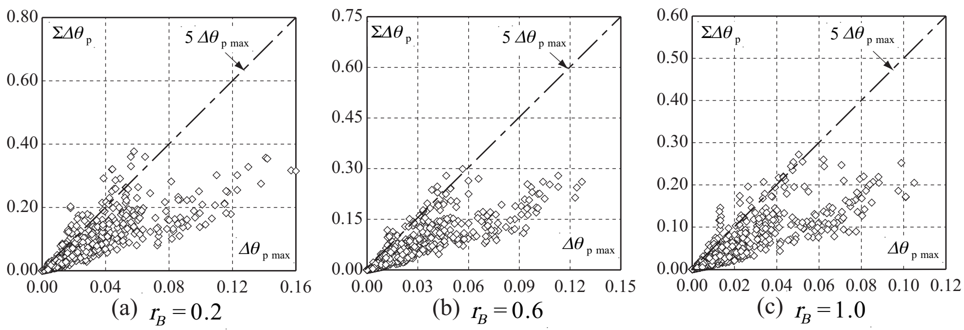

Figure 3.10: Relationship between $\Sigma\Delta\theta_p$ and $\Delta\theta_{p\,\max}$ of the Second-Floor Beam End

4. CONCLUSION

In this paper, we aim for the establishment of a method to evaluate the ductility demand of beam ends and column bases when the maximum story drift angle ($R_{\max}$) under earthquakes was specified. The rotational springs were inserted into the column base of 15 steel moment frames that were fabricated according to the Japanese seismic design code. In addition, the relationship between the plastic deformation of the column base or the second-floor beam end and maximum story drift angle was described. The results are summarized as

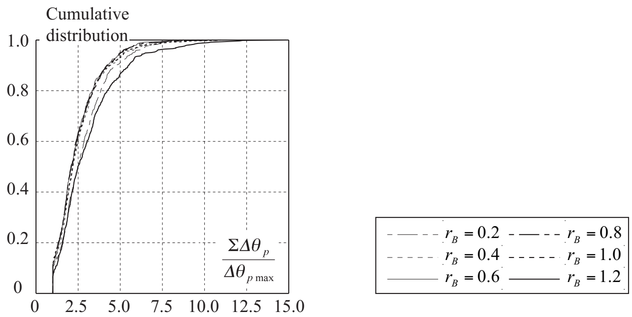

Figure 3.11: Cumulative Distribution $\Sigma\Delta\theta_p / \Delta\theta_{p\max}$ of the Second-Floor Beam End

follows.

(1) The maximum plastic rotation ($\theta_{p\max}$) of the column base can be approximated as follows even if the strength of the column base is changed.

$$_{pre\,c}\theta_{p\max} \cong \min\left\{1.5\left(R_{\max} - R_y\right), 1.5\left(R_C - R_y\right) + R_{\max} - R_C\right\} \tag{4.1}$$

R_C is the story drift angle when the top of the column of the first story yields, and can be approximated as follows using the ultimate base shear coefficient (C_B) and base shear coefficient of the elastic limit (C_y).

$$R_C = \left(\frac{C_B - C_y}{0.4C_y} + 1\right) R_y \tag{4.2}$$

(2) The maximum increment of the plastic rotation ($\Delta\theta_{p\max}$) of the column base is between 1.0 times and twice of the maximum plastic rotation ($\theta_{p\max}$) of the column base.

$$1.0\,\theta_{p\max} < \Delta\theta_{p\max} < 2.0\,\theta_{p\max} \tag{4.3}$$

(3) $\Delta\theta_{p\max} / \theta_{p\max}$ of the column base increases as the strength of the column base decreases.
(4) $\Sigma\Delta\theta_p / \Delta\theta_{p\max}$ of the column base increases rapidly as the strength of the column base decreases.
(5) The plastic deformation of the second-floor beam end is not influenced by a decrease in the strength of the column base.

REFERENCES

Nakahara, H., Yamanari, M., and Ogawa, K. (2005). Plastic deformation of beam in steel moment-resistant frames subjected to strong earthquake. *Proceedings of International Conference on Advances on Steel Structures* **1:I**, 203-208

Kawano, A. (1998). Inelastic response behavior of steel frame considered restoring force characteristics of column-base. *Proceedings of Fifth Pacific Structural Steel Conference* **1**, 117-122

Kawano, A., Tanaka, Y., and Matsui, C. (2000). Earthquake response behavior of multi-story weak-beam-frames including restoring force characteristics of first floors column-base. *Proceedings of 6th ASCCS Conference, Composite and Hybrid Structures* **1**, 151-158

Somerville P. et al. (1997). Development of ground motion time histories for phase 2 of the FEMA/SAC steel project. *Report No.SAC/BD-97-04, SAC Joint Venture*

Inoue, K., Ogawa, K., and Kamura, H. (1999). Modeling of the moment frame to fishbone-shaped frame for the earthquake response analysis. *Proceedings of the 1999 Structures Congress*, SEI of ASCE, 414-417